Robust Power Control with Distribution Uncertainty in Cognitive Radio Networks

Shimin Gong*, Ping Wang*, Yongkang Liu†, Weihua Zhuang†
* Nanyang Technological University, Singapore
†University of Waterloo, Canada

Abstract – In cognitive radio networks, it is often impossible to have regular information exchange between PUs and SUs. This implies that SUs are unable to obtain up-to-date channel information at the PU side, and will face technical challenges in accurately controlling their interference to PUs through power control. In this paper, we assume that SUs can estimate the channel information in the reciprocal channel, and study the channel uncertainty due to estimation errors and its impact on SUs' performance and PUs' protection. Specifically, we model the uncertain channel gain to be a random variable following a state-dependent distribution function, and propose a power control mechanism that is robust against the channel uncertainty. We study the robust power control in two cases. In the first case, all SU transmitters (e.g., secondary base stations) transmit with the same power, while in the second case each SU transmitter may choose distinct transmit power based on its own preference. In either case, we formulate the power control problem as a chance constrained robust optimization problem and design an iterative algorithm, respectively. Numerical results show that our robust power control mechanism can provide better protection for PUs than existing methods that overlook the uncertainty in channel measurement, and the second-case power control generally provides better Quality of Service (QoS) for SUs than that in the first case.

Index Terms – Cognitive power control, robust optimization, distribution uncertainty, probabilistic distance measure, concave-convex procedure.

I. Introduction

Cognitive radio networks [1] allow the unlicensed secondary users (SUs) to access temporarily unused channels as long as they do not generate unacceptable interference to the legacy licensed primary users (PUs). On one hand, limiting interference to PUs is dictated by spectrum regulations to protect the license holder; on the other hand, it is desired for SUs to maximize their overall performance. Excessive interference usually causes transmission failures and requires additional spectrum opportunities for retransmission. Therefore, effective interference management is required at the SU side, and in general contains two aspects, i.e., interference awareness and interference mitigation. Interference awareness refers to the detection of potential active PUs and the estimation of interference at PU receivers. So far, most of the spectrum sensing algorithms focus on detecting PU transmitters with limited considerations in estimating the interference at PU receivers. Interference mitigation uses a coordination mechanism among SUs as well as the PUs in a centralized or decentralized manner, so as to mitigate mutual interference and improve SUs' performance. It can be achieved in different ways. In a single channel case, power control is used to maximize SUs' overall performance subject to an interference constraint at the PU side [2], [3]. While in a multi-channel case, individual SU can first choose the operating channel and then perform a power control algorithm to avoid severe interference with the SUs and PUs on the same channel [4], [5]. Our work in this paper mainly focuses on the power control problem.

One main challenge is that interference awareness is hardly reliable in practice due to errors in channel estimation. Konrad *et al.* demonstrate in [6] that channel characteristics exhibit time-varying effects in a long time period, which is caused by the change of *physical channel conditions*, e.g., a light-of-sight (LOS) path between transceivers may exist for some time and disappear when the path is blocked temporarily. To make accurate estimation, the physical channel conditions should remain stable for a sufficient time to provide enough channel samples. Let *static period* denote a small time duration in which SUs remain stationary and physical channel conditions do not change. However, such a static period may be very short due to user mobility, resulting in very limited data samples for channel estimation. Moreover, SUs are generally unable to detect when a static period starts or how long it lasts due to their hardware-constrained sensing capabilities. Therefore, the channel samples may stem from different static periods, which gives inaccurate channel information in different static periods.

Channel uncertainty may also originate from the lack of regular information exchange between SUs and PUs. As a result, the interference information at PU receivers cannot be fed back to SU transmitters on time. Some existing works assume a prior knowledge of SUs' locations or spatial distribution, based on which SUs can estimate the interference at PU receivers using a signal propagation model [2], [7]. However, these assumptions are not practical as they usually imply a site survey before the deployment of a secondary network. Besides, the interference estimation based on theoretical propagation models is usually oversimplified and very different from reality. Another recently proposed method is to estimate the reciprocal channel by overhearing feedback from PU receivers [8], [9]. This method may be unreliable for real-time power control due to limited observations of feedback from PU receivers. Specifically, PU receivers may send feedback (e.g., ACK packets) sporadically after receiving a bulk of data streaming, thus channel estimation in this way may not capture the changes of channel character-

istics timely. If power control is based on out-of-date channel estimates, SUs cannot know the actual interference at the PU receivers, which will lead to violations of PUs' interference constraints, especially when channel gain changes over time.

To avoid excessive interference caused by channel uncertainty, some power control methods are proposed to deal with channel gain fluctuations by modeling the channel gain as a combination of deterministic and uncertain components. In general, these methods fall into two approaches, i.e., stochastic and the worst-case approaches. A *stochastic approach* assumes the uncertain component to follow a known distribution function, which usually leads to chance constraints in the power control problem. For implementation simplicity, the chance constraints are further transformed into convex forms. Zheng *et al.* in [10] consider the uncertain component as Gaussian noise and convert interference outage probability into a generalized Marcum's Q function [11]. In a similiar way, Dall'Anese *et al.* in [12] approximate PUs' aggregate interference power (AIP) levels and SUs' signal to noise and interference ratios (SINRs) as log-normal distributed random variables, and then solve the resulting problem via sequential geometric programming. The challenge of a stochastic approach lies in the assumption of a known distribution function, which is often unavailable, or is very pricey to obtain in practice. Hence, some other works employ a *worst-case approach* that merely restricts the fluctuations of the uncertain component to be within a bounded and convex set. Zheng *et al.* in [13] describe the uncertain component by an ellipsoid in terms of channel quality or covariance matrix, and approximate the power control problem into a semi-definite program (SDP) based on rank relaxation, which can be solved by two randomized algorithms proposed in [14]. Compared with the stochastic approach and other non-robust methods that assume full knowledge of the channel gain, the worst-case approach can provide the highest PU protection level, however, with the price of conservative performance for SU transmissions.

In this paper, we describe the channel uncertainty in a novel model that sidesteps the difficulties in obtaining exact distribution functions for AIP and SINR [10], [12], [15], and the difficulties in choosing appropriate bounding set in the worst-case approach [13], [14]. This new model makes use of channel measurement history, but not completely relies on it. Our approach is a combination of the stochastic and the worst-case approaches, which bears several contributions as follows:

- *Channel Uncertainty Model*- Based on historical channel measurements, we extract closed-form approximations for AIP and SINR distributions, and use them as reference distributions. Considering various uncertain factors in practice, we allow the actual distributions of AIP and SINR to deviate from their reference distributions, respectively, and characterize their differences by a probabilistic distance measure. To the best of our knowledge, this is the first work that deals with uncertain distributions of AIP and SINR in power control for cognitive radio networks.
- *Robust Optimization & Iterative Algorithm*- We formulate a chance constrained robust optimization that takes distribution functions as the uncertain variables, and develop an iterative algorithm to search for the optimal transmit power. For the case in which all SUs have the same transmit power, we first find the worst-case AIPs at PU receivers with fixed transmit power, and then update the transmit power using a bisection method until the interference requirement is met at PU receivers. For the second case in which each user may choose its own transmit power, it becomes a non-convex problem and we develop a heuristic algorithm that allows each user to iteratively maximize its own utility. Simulation results show that the heuristic algorithm for the second case provides better QoS for SUs than the bisection method in the first case, however, at the cost of higher computational complexity.

The remainder of this paper is organized as follows. Section II describes the channel model, performance metrics, and the new uncertainty model. Section III and IV present two iterative algorithms for the power control in two different cases, respectively. In Sections V and VI, we present some numerical results and draw the conclusions.

II. System Model

We consider a cognitive radio network consisting of M PUs spatially distributed in the coverage area of a primary base station (PBS), and K secondary access points (SAPs) serving N SUs in an *underlay* manner (as shown in Fig. 1), sharing the same spectrum band with the primary network simultaneously conditioned on limited interference to PUs. Both primary and secondary networks mainly provide down-link data streaming services, e.g., file downloading and video streaming. Therefore, data transmissions are mainly from the PBS and SAPs to PUs and SUs, respectively. The sets of PUs, SUs and SAPs are denoted by $\mathcal{M}$, $\mathcal{N}$ and $\mathcal{K}$, respectively. Let $\mathcal{N}_k$ be the set of SUs associated with SAP k. Assume $\mathcal{N} = \bigcup_{k\in\mathcal{K}} \mathcal{N}_k$ and $\mathcal{N}_i \bigcap \mathcal{N}_j = \emptyset$ for any $i, j \in \mathcal{K}$ and $i \neq j$. There is no direct information exchange between SUs and PUs, but a common control channel among SAPs to coordinate with each other and share channel sensing information [16]. After information sharing and processing, the SAPs perform necessary adjustments on transmit power to maximize overall performance of the secondary network, as well as to prevent excessive interference to the primary network. PUs and SUs can be mobile users with relatively low mobility as compared with the convergence speed of a power control algorithm. That is, user mobility does not incur a new round of power adjustments before the convergence of previous adjustments.

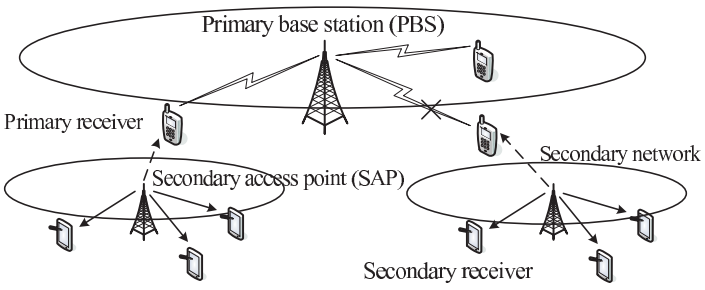

Fig. 1: Network model

A. Time-varying Channel Model

In wireless communications, the channel gain is a composite effect of small-scale fading and large-scale path loss, and time-varying as demonstrated in [6]. Over a small time period with fixed physical channel conditions, the channel effects can be captured as a stationary process and we can characterize AIP and SINR by stationary distribution functions, which may change correspondingly if physical channel conditions have changed. Therefore, we model the time-varying channel effects as concatenations of piecewise stationary processes [17]. Each stationary process corresponds to a channel state S_z that is defined by the stationary distributions of AIP ϕ_m for $m \in \mathcal{M}$ and SINR γ_n for $n \in \mathcal{N}$ (Specific forms of AIP ϕ_m and SINR γ_n are to be explained in next section), i.e., $S_z = (f^z_{\phi_1}(x), \ldots, f^z_{\phi_M}(x), f^z_{\gamma_1}(x), \ldots, f^z_{\gamma_N}(x))$ where $f^z_{\phi_m}(x)$ and $f^z_{\gamma_n}(x)$ denote the pdfs of AIP ϕ_m and SINR γ_n, respectively for state z. Variations of the physical channel conditions result in the transitions between different states. In Fig. 2, we present a 2-state example. A LOS path between SAP and PU m may exist (e.g., state S_1) for some time and the channel gain follows a Rician distribution, which is different from the Rayleigh distribution when direct transmissions are blocked by surrounding obstructions (e.g., state S_2). Therefore, distributions $f^1_{\phi_m}(x)$ and $f^2_{\phi_m}(x)$ take different forms since AIP ϕ_m is a composite random variable of the channel gain.

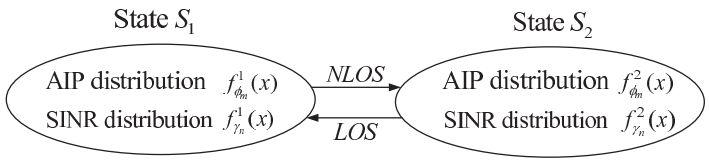

Fig. 2: Non-stationary channel model with two states.

B. Stochastic PU Protection and QoS Provisioning

For each state in Fig. 2 during a static period, let g_{km} denote the channel gain from SAP k to PU m, and h_{kn} the channel gain from SAP k to SU n. When SAP k transmits with power p_k, the AIP at PU $m \in \mathcal{M}$ is given by $\phi_m = \sum_{k=1}^{K} p_k g_{km}$, and the instantaneous SINR at SU $n \in \mathcal{N}_k$ is $\gamma_n = \frac{p_k h_{kn}}{\sigma_n^2 + \pi_n + \sum_{s=1, s\neq k}^{K} p_s h_{sn}}$, where σ_n^2 is the noise power received by SU n and π_n denotes the PBS' interference to SU n. Note that the SINR and AIP are composite random variables of the channel gains $\{h_{kn}\}$ and $\{g_{km}\}$, respectively. We characterize PU's interference by an outage probability that AIP is greater than a threshold $\bar{\phi}_m$. Define the stochastic PU protection as the outage probability, for each PU $m \in \mathcal{M}$, to be bounded by a maximum acceptable value η_m, i.e., $\mathbb{P}\{\phi_m \geq \bar{\phi}_m\} \leq \eta_m$, where $\bar{\phi}_m$ is the maximum interference acceptable by a PU receiver (i.e., interference threshold) and $\mathbb{P}\{A\}$ denotes the probability of event A. For an SU n, we consider its transmission failed if the received SINR γ_n is less than a minimum QoS threshold $\bar{\gamma}_n$. Correspondingly, we define the service rate of each SU as the probability of its successful reception, i.e., $\mathbb{P}\{\gamma_n \geq \bar{\gamma}_n\}$. Then, the stochastic QoS provisioning for SUs is to maximize the average service rate of all SUs, subject to a stochastic PU protection level:

$$\max_{\boldsymbol{p}} \quad \sum_{n\in\mathcal{N}} \omega_n \mathbb{P}\{\gamma_n \geq \bar{\gamma}_n\} \tag{1a}$$

$$s.t. \quad \mathbb{P}\{\phi_m \geq \bar{\phi}_m\} \leq \eta_m, \quad m \in \mathcal{M} \tag{1b}$$

$$0 \leq p_k \leq \bar{p}_k, \quad k \in \mathcal{K} \tag{1c}$$

where $\boldsymbol{p} = [p_1, p_2, \ldots, p_K]$ denotes the transmit power of SAPs, and $\bar{p}_k$ is the maximum transmit power of SAP k. Different weights $\{\omega_n\}_{n\in\mathcal{N}}$ represent service priorities associated with different SUs. Most existing works address the problem (1a)-(1c) with known channel states and look for closed-form approximations for the distributions of AIP and SINR so as to convert problem (1a)-(1c) into a convex form [12]. However, it is a challenging issue since SAPs are in general unable to detect the state transitions due to their hardware-constrained sensing capabilities. It usually requires sufficient data samples to have accurate channel estimation, which is often unavailable due to limited sensing time and sample size. Besides, the estimation of AIP requires SAPs to listen to the feedback from PU receivers, which are generally sporadic and cannot provide real-time channel information.

C. Distribution Uncertainty

The SAPs' blindness to channel state transitions requires SAPs to use a power strategy that is robust against the distribution uncertainty. Robustness implies that once we have a feasible power strategy for state S_1 as in Fig. 2, it should still be able to provide the required PU protection level when channel state transits to S_2. To achieve this, we first develop a quantitative way to study how the distributions of AIP and SINR may change with time. Through channel measurement, we can obtain closed-form approximations for the AIP and SINR distributions by goodness-of-fit tests. Different from existing works, we view these approximations only as reference distributions of AIP and SINR, their actual distributions can differ from the references in the next sensing period. Let $f^0_{\gamma_n}(x)$ and $f^0_{\phi_m}(x)$ be the reference distributions of SINR γ_n and AIP ϕ_m, respectively, and simply denote $f^z_{\gamma_n}(x)$ (or $f^z_{\phi_m}(x)$, respectively) as $f_{\gamma_n}(x)$ (or $f_{\phi_m}(x)$, respectively) since channel state z is uncertain to SAPs. We quantify the difference between the actual distribution $f_{\gamma_n}(x)$ and its reference $f^0_{\gamma_n}(x)$ by a probabilistic distance measure, i.e., the Kullback-Leibler (KL) divergence [18]:

$$D_{KL}(f_{\gamma_n}(x), f^0_{\gamma_n}(x)) = \mathbb{E}_{f_{\gamma_n}}\left[\ln f_{\gamma_n}(x) - \ln f^0_{\gamma_n}(x)\right].$$

The KL divergence is a non-symmetric measure of the difference between two probability density functions. Here, $f_{\gamma_n}(x)$ represents the real distribution of data through long term observation and precise modeling, while $f^0_{\gamma_n}(x)$ is a closed-form approximation based on theoretic assumptions and simplifications. The divergence characterizes the logarithmic difference between distributions $f_{\gamma_n}(x)$ and $f^0_{\gamma_n}(x)$, averaged by distribution $f_{\gamma_n}(x)$. When these two distributions are similar to each other, the distance measure is close to zero. Then, we can define the distribution uncertainty for γ_n as

$$\mathbb{Z}_{\gamma_n}(f^0_{\gamma_n}(x), D_{\gamma_n}) = \{f_{\gamma_n}(x) \,|\, D_{KL}(f_{\gamma_n}, f^0_{\gamma_n}) \leq D_{\gamma_n}\}$$

where D_{γ_n} represents a distance limit that bounds the probabilistic difference between $f^0_{\gamma_n}(x)$ and $f_{\gamma_n}(x)$. It can be set properly based on historical channel measurements. Similarly, we can define the distribution uncertainty $\mathbb{Z}_{\phi_m}(f^0_{\phi_m}(x), D_{\phi_m})$ for AIP ϕ_m. In practice, we can set both $f^0_{\gamma_n}(x)$ and $f^0_{\phi_m}(x)$ as log-normal distributions [12] and update them online if real-time measurements indicate large deviations, in terms of KL divergence, from their reference distributions.

III. Case I: SAPs Transmit with the Same Power

Given the uncertainty sets $\{\mathbb{Z}_{\gamma_n}\}_{n\in\mathcal{N}}$ and $\{\mathbb{Z}_{\phi_m}\}_{m\in\mathcal{M}}$, the robust power control problem in (1a)-(1c) is rewritten as:

$$\max_{\boldsymbol{p}} \min_{f_{\boldsymbol{\gamma}}\in\mathbb{Z}_{\boldsymbol{\gamma}}} \sum_{n\in\mathcal{N}} \omega_n \mathbb{E}_{f_{\gamma_n}}[\mathbf{1}(x \geq \bar{\gamma}_n)] \tag{2a}$$

$$s.t. \max_{f_{\phi_m}\in\mathbb{Z}_{\phi_m}} \mathbb{E}_{f_{\phi_m}}[\mathbf{1}(x \geq \bar{\phi}_m)] \leq \eta_m, \quad m \in \mathcal{M} \tag{2b}$$

$$\mathbf{0} \preceq \boldsymbol{p} \preceq \bar{\boldsymbol{p}} \tag{2c}$$

where $f_{\boldsymbol{\gamma}}(\boldsymbol{x})$ is a joint distribution function of $\{\gamma_n\}$, $n \in \mathcal{N}$ and $\mathbb{Z}_{\boldsymbol{\gamma}} \triangleq \prod_{n\in\mathcal{N}} \mathbb{Z}_{\gamma_n}$. $\mathbf{1}(A)$ is an indicator function which equals 1 if event A is true and 0 otherwise. The service rate in (1a) and outage probability in (1b) are represented by expectation functions (denoted by $\mathbb{E}[\cdot]$) averaged over distributions $f_{\gamma_n}(x)$ and $f_{\phi_m}(x)$, respectively. Our objective is to optimize the transmit power at each SAP, so as to maximize the worst-case QoS provisioning for SUs, while maintaining prescribed PU protection level even under worst-case channel conditions.

Note that constraint (2b) requires every PU, $m \in \mathcal{M}$, to be protected by a probability η_m. When all PUs have the same protection levels, i.e., $\eta_1 = \cdots \eta_M = \eta$, we only need to focus on the most vulnerable PU, which experiences a worst-case channel condition [15]. If the most vulnerable PU is protected by η, other PUs can be better protected. Let the $\tilde{m}$ denote the most vulnerable PU, constraint (2b) is equivalent to

$$\max_{f_{\phi_{\tilde{m}}}} \mathbb{E}_{f_{\phi_{\tilde{m}}}}[\mathbf{1}(x \geq \bar{\phi}_{\tilde{m}})] \leq \eta. \tag{3}$$

Constraint (2b) or (3) is suitable for per-node based power control [15], [19] and data packet is delivered through multiple hops. Within one hop distance, two neighboring SU transceivers can transmit with very low power so as to limit their interference to the most vulnerable PU receiver.

On the other hand, this constraint is rather conservative in our broadcast model where the data streaming are mainly from SAPs to SUs [2]. Each SAP tries to maximize its coverage area and serve more SUs. But once a PU receiver moves very close to a SAP and experiences high interference, constraint (3) will prevent the SAP from serving all associated SUs. For better service in the secondary network, we emphasize on the interference to the whole primary network, rather than to an individual receiver. That is, though PUs may experience different protection levels, the average protection for all PUs is maintained at a constant level η. As a result, we define a new interference constraint as

$$\max_{f_{\boldsymbol{\phi}}\in\mathbb{Z}_{\boldsymbol{\phi}}} \frac{1}{M} \sum_{m\in\mathcal{M}} \mathbb{E}_{f_{\phi_m}}[\mathbf{1}(x \geq \bar{\phi}_m)] \leq \eta \tag{4}$$

where $f_{\boldsymbol{\phi}}(\boldsymbol{x})$ is the joint distribution function of $\{\phi_m\}$, $m \in \mathcal{M}$ and $\mathbb{Z}_{\boldsymbol{\phi}} \triangleq \prod_{m\in\mathcal{M}} \mathbb{Z}_{\phi_m}$. Assuming AIPs ϕ_m are independent random variables at different PUs, (4) is equivalent to

$$\frac{1}{M} \sum_{m\in\mathcal{M}} \max_{f_{\phi_m}} \mathbb{E}_{f_{\phi_m}}[\mathbf{1}(x \geq \bar{\phi}_m)] \leq \eta.$$

Here, we consider all SAPs transmitting with the same power level, i.e., $p_1 = \ldots p_K = p_s$. As a result, the robust power control with constraint (4) has only one control variable. It is easy to prove that both objective (2a) and the LHS of (4) are increasing functions of the transmit power p_s. Therefore, optimal transmit power p_s can be uniquely determined by the equality condition of constraint (4). In order to check whether constraint (4) is satisfied with a given transmit power p_s, we need to solve, for each $m \in \mathcal{M}$, a robust optimization problem as follows:

$$\max_{f_{\phi_m}} \quad \mathbb{E}_{f_{\phi_m}}[\mathbf{1}(x \geq \bar{\phi}_m)] \tag{5a}$$

$$s.t. \quad \mathbb{E}_{f_{\phi_m}}\left[\ln f_{\phi_m}(x) - \ln f^0_{\phi_m}(x)\right] \leq D_{\phi_m} \tag{5b}$$

$$\mathbb{E}_{f_{\phi_m}}[1] = 1. \tag{5c}$$

Constraint (5b) defines the distribution uncertainty of AIP ϕ_m, and (5c) restricts $f_{\phi_m}(x)$ to be a valid probability density distribution function. Though we focus on constraint (4), note that the formulation in (5a)-(5c) can also be used to study (3).

Let $\eta^w_m(p_s) = \max_{f_{\phi_m}} \mathbb{E}_{f_{\phi_m}}[\mathbf{1}(x \geq \bar{\phi}_m)]$ denote the worst-case interference at PU receiver m when SAPs transmit with power p_s. By the Lagrangian method, we have

$$\begin{aligned}\eta^w_m(p_s) \quad = \quad & \min_{\tau_m,\lambda_m} \max_{f_{\phi_m}} \mathbb{E}_{f_{\phi_m}}\left[\mathbf{1}(x \geq \bar{\phi}_m) - \lambda_m\right] + \lambda_m \\ & -\tau_m \mathbb{E}_{f_{\phi_m}}[\ln f_{\phi_m}(x) - \ln f^0_{\phi_m}(x)] + \tau_m D_{\phi_m}\end{aligned}$$

where non-negative τ_m and λ_m denote the Lagrangian multipliers associated with constraints (5b) and (5c), respectively. Let $\mathcal{P}(p_s, f_{\phi_m}, \tau_m, \lambda_m) = \mathbb{E}_{f_{\phi_m}}\left[\mathbf{1}(x \geq \bar{\phi}_m) - \lambda_m - \tau_m \ln \frac{f_{\phi_m}(x)}{f^0_{\phi_m}(x)}\right]$. The derivative of $\mathcal{P}(p_s, f_{\phi_m}, \tau_m, \lambda_m)$ with respect to f_{ϕ_m} is given by

$$\frac{\partial \mathcal{P}}{\partial f_{\phi_m}} = \int_{x\in S} \left(\mathbf{1}(x \geq \bar{\phi}_m) - \tau_m \ln \frac{f_{\phi_m}(x)}{f^0_{\phi_m}(x)} - \tau_m - \lambda_m\right) dx$$

where S denotes the set of all possible observations of AIP ϕ_m. By the Karush-Kuhn-Tucker (KKT) condition, we have

$$\mathbf{1}(x \geq \bar{\phi}_m) - \tau_m \ln \frac{f_{\phi_m}(x)}{f^0_{\phi_m}(x)} - \tau_m - \lambda_m = 0 \tag{6a}$$

$$\int_{x\in S} f_{\phi_m}(x)\, dx = 1 \tag{6b}$$

$$D_{\phi_m} - \mathbb{E}_{f_{\phi_m}}\left[\ln \frac{f_{\phi_m}(x)}{f^0_{\phi_m}(x)}\right] \geq 0 \tag{6c}$$

$$\tau_m \left(D_{\phi_m} - \mathbb{E}_{f_{\phi_m}}\left[\ln \frac{f_{\phi_m}(x)}{f^0_{\phi_m}(x)}\right]\right) = 0. \tag{6d}$$

From (6a), the worst-case distribution function is given by

$$f^*_{\phi_m}(x) = f^0_{\phi_m}(x) \exp\left(\frac{\mathbf{1}(x \geq \bar{\phi}_m) - \lambda_m}{\tau_m} - 1\right) \tag{7}$$

where (τ_m, λ_m) satisfies conditions (6b)-(6d). Specifically, we have the following proposition.

Proposition 1: The choice of (τ_m, λ_m) is a solution to the following nonlinear equations

$$\begin{aligned} H_1(\tau_m, \lambda_m) &\triangleq R(\bar{\phi}_m)e^{-\frac{\lambda_m}{\tau_m}} + S(\bar{\phi}_m)e^{\frac{1-\lambda_m}{\tau_m}} - 1 = 0 \\ H_2(\tau_m, \lambda_m) &\triangleq S(\bar{\phi}_m)e^{\frac{1-\lambda_m}{\tau_m}} - \lambda_m - \tau_m(1 + D_{\phi_m}) = 0 \end{aligned}$$

where $S(\bar{\phi}_m) = \left(1 - \mathcal{G}(\bar{\phi}_m)\right)e^{-1}$, $R(\bar{\phi}_m) = \mathcal{G}(\bar{\phi}_m)e^{-1}$, and $\mathcal{G}_n(\bar{\phi}_m) = \int_{x<\bar{\phi}_m} f^0_{\phi_m}(x)\,dx$.

Proof: The proof is straightforward by substituting distribution $f^*_{\phi_m}(x)$ in (7) to conditions (6b)-(6d). Note that (6c) always holds when we have (6d) and $\tau_m \geq 0$. From (6b), we have

$$\begin{aligned} \int_{x\in S} f^*_{\phi_m}(x)\,dx &= \int_{x<\bar{\phi}_m} f^0_{\phi_m}(x)e^{-\frac{\lambda_m}{\tau_m}-1}\,dx \\ &\quad + \int_{x\geq\bar{\phi}_m} f^0_{\phi_m}(x)e^{\frac{1-\lambda_m}{\tau_m}-1}\,dx \\ &= R(\bar{\phi}_m)e^{-\frac{\lambda_m}{\tau_m}} + S(\bar{\phi}_m)e^{\frac{1-\lambda_m}{\tau_m}} = 1 \end{aligned}$$

Thus we have $H_1(\tau_m, \lambda_m) = 0$. Similarly for (6d), we have

$$\mathbb{E}_{f^*_{\phi_m}}\left[\ln\frac{f_{\phi_m}(x)}{f^0_{\phi_m}(x)}\right] = \frac{\mathbb{E}_{f^*_{\phi_m}}[\mathbf{1}(x \geq \bar{\phi}_m)] - \lambda_m}{\tau_m} - 1,$$

and it is equivalent to

$$\begin{aligned} \tau_m D_n &= \mathbb{E}_{f^*_{\phi_m}}[\mathbf{1}(x \geq \bar{\phi}_m)] - \lambda_m - \tau_m \\ &= \int_{x\geq\bar{\phi}_m} f^0_{\phi_m}(x)e^{\frac{1-\lambda_m}{\tau_m}-1}\,dx - \lambda_m - \tau_m \\ &= S(\bar{\phi}_m)e^{\frac{1-\lambda_m}{\tau_m}} - \lambda_m - \tau_m \end{aligned}$$

which implies $H_2(\tau_m, \lambda_m) = 0$. ∎

A direct solution to these nonlinear equations is difficult to obtain. Thus, we resort to an iterative method. Firstly, we take linear approximations for $H_1(\tau_m, \lambda_m)$ and $H_2(\tau_m, \lambda_m)$ as follows:

$$\begin{bmatrix} H_1(\tau_m^{'}, \lambda_m^{'}) \\ H_2(\tau_m^{'}, \lambda_m^{'}) \end{bmatrix} \approx \begin{bmatrix} H_1(\tau_m, \lambda_m) \\ H_2(\tau_m, \lambda_m) \end{bmatrix} + \boldsymbol{J}(\tau_m, \lambda_m)\begin{bmatrix} \Delta\tau_m \\ \Delta\lambda_m \end{bmatrix}$$

where $\tau_m^{'} = \tau_m + \Delta\tau_m$, $\lambda_m^{'} = \lambda_m + \Delta\lambda_m$, and $\boldsymbol{J}(\tau_m, \lambda_m)$ denotes the Jacobian matrix evaluated at (τ_m, λ_m). Then we find an update for (τ_m, λ_m) if it is not feasible. The update $[\Delta\tau_m, \Delta\lambda_m]^T$ is a solution to the linear equation $\boldsymbol{J}(\tau_m, \lambda_m)\begin{bmatrix} \Delta\tau_m \\ \Delta\lambda_m \end{bmatrix} = -\begin{bmatrix} H_1(\tau_m, \lambda_m) \\ H_2(\tau_m, \lambda_m) \end{bmatrix}$. Note that τ_m should be non-negative during iterations.

Once we determine (τ_m, λ_m) for each PU receiver m, we can check the feasibility of p_s by comparing $\sum_{m\in\mathcal{M}} \eta^w_m(p_s)$ and the target η, where $\eta^w_m(p_s) = \mathbb{E}_{f^*_{\phi_m}}[\mathbf{1}(x \geq \bar{\phi}_m)] = (1 + D_{\phi_m})\tau_m + \lambda_m$. The second equality is obtained from (6a) and (6d). Next, we will find the optimal transmit power p^*_s such that $\sum_{m\in\mathcal{M}} \eta^w_m(p^*_s) = \eta$. Note that $\eta^w_m(p_s)$ is an increasing function with respect to p_s since we have

$$\begin{aligned} \partial\eta^w_m(p_s)/\partial p_s &= \frac{\partial}{\partial p_s}\int_{\bar{\phi}_m}^{\infty} f^*_{\phi_m}(x)\,dx \\ &= \frac{\partial}{\partial p_s}\int_{\bar{\phi}_m/p_s}^{\infty} f^*_{z_m}(x)\,dx = \frac{\bar{\phi}_m}{p_s^2} f^*_{z_m}(\frac{\bar{\phi}_m}{p_s}) > 0 \end{aligned}$$

where $z_m = \sum_{k\in\mathcal{K}} g_{km} = \phi_m/p_s$ is the aggregated channel gain and thus follows a distribution $f^*_{z_m}(x) = f^*_{\phi_m}(xp_s)p_s$ in the worst-case. The monotonicity of $\eta^w_m(p_s)$ allows us to search for p^*_s using a bisection method [20]. With this transmit power p^*_s, objective (2a) gives a lower bound of the stochastic QoS provisioning for SUs, and can be processed in the same way as that for problem (5a)-(5c) when user priorities $\{\omega_n\}_{n\in\mathcal{N}}$ are fixed.

IV. Case II: SAPs Transmit with Distinct Power

In the second case, each SAP adjusts its own transmit power so that its own utility (to be discussed) can be maximized. Considering SAPs' spatial distribution and different influences to the PUs, it is likely that they have distinct transmit power levels at optimum. Note that the uncertainty in SUs' SINR γ_n can be processed in the same way as for AIP ϕ_m. Therefore, we only consider the uncertainty set $\mathbb{Z}_{\phi_m}$ in the following. Let $F_{n_k}(\bar{\gamma}_{n_k}, p_k) = \mathbb{E}_{f_{\gamma_{n_k}}}[\mathbf{1}(x \geq \bar{\gamma}_{n_k})]$ denote the service rate of SU n_k, where $f_{\gamma_{n_k}}(\cdot)$ is a known log-normal distribution. Then, each SAP's utility is the weighted sum of service rates of all associated SUs and is given by $u_k(\boldsymbol{p}_{-k}, p_k) = \sum_{n_k\in\mathcal{N}_k} \omega_{n_k} F_{n_k}(\bar{\gamma}_{n_k}, p_k)$, where $\boldsymbol{p}_{-k}$ denotes the power levels for all SAPs other than SAP k. Then our target is to determine the transmit power $\boldsymbol{p}$ for the following optimization problem:

$$\max_{\boldsymbol{p}} \quad \sum_{k\in\mathcal{K}} u_k(\boldsymbol{p}_{-k}, p_k) \tag{8a}$$

$$s.t. \quad I(\boldsymbol{p}_{-k}, p_k) \leq \eta \tag{8b}$$

where $I(\boldsymbol{p}_{-k}, p_k) \triangleq \frac{1}{M}\sum_{m\in\mathcal{M}} \max_{f_{\phi_m}\in\mathbb{Z}_{\phi_m}} \mathbb{E}_{f_{\phi_m}}[\mathbf{1}(x \geq \bar{\phi}_m)]$ denotes PUs' average outage probability when SAPs transmit with power $\boldsymbol{p}$.

Proposition 2: SAP's utility $u_k(\boldsymbol{p}_{-k}, p_k)$ and PUs' interference $I(\boldsymbol{p}_{-k}, p_k)$ are both concave functions of p_k.

Proof: As utility $u_k(\boldsymbol{p}_{-k}, p_k)$ is a weighted summation of $F_{n_k}(\bar{\gamma}_{n_k}, p_k)$ for each user $n_k \in \mathcal{N}_k$, our focus shifts to study the concavity of function $F_{n_k}(\bar{\gamma}_{n_k}, p_k)$. Let $g_{kn} = \frac{h_{kn}}{n_0 + \sum_{i\neq k} p_i h_{in}}$ and $f_g(x)$ be the distribution of g_{kn}. With $\gamma_{n_k} = p_k g_{kn}$, given the distribution $f_{\gamma_{n_k}}(x)$ of γ_{n_k}, we have $f_g(x) = p_k f_{\gamma_{n_k}}(p_k x)$ and $F_{n_k}(\bar{\gamma}_{n_k}, p_k) = \int_{\bar{\gamma}_{n_k}}^{\infty} f_{\gamma_{n_k}}(x)\,dx = \int_{\frac{\bar{\gamma}_{n_k}}{p_k}}^{\infty} f_g(x)\,dx$. Therefore,

$$\partial F_{n_k}(\bar{\gamma}_{n_k}, p_k)/\partial p_k = f_g(\frac{\bar{\gamma}_{n_k}}{p_k})\frac{\bar{\gamma}_{n_k}}{p_k^2} \geq 0, \tag{9}$$

and its second-order derivative with respect to p_k is give by

$$\begin{aligned} \frac{\partial^2 F_{n_k}}{\partial p_k^2} &= -\frac{\bar{\gamma}_{n_k}}{p_k^3}\left(2f_g(\frac{\bar{\gamma}_{n_k}}{p_k}) + \frac{\bar{\gamma}_{n_k}}{p_k}f_g^{'}(\frac{\bar{\gamma}_{n_k}}{p_k})\right) \\ &= -\frac{\bar{\gamma}_{n_k}}{p_k^2}\left(2f_{\gamma_{n_k}}(\bar{\gamma}_{n_k}) + \bar{\gamma}_{n_k}f^{'}_{\gamma_{n_k}}(\bar{\gamma}_{n_k})\right). \end{aligned} \tag{10}$$

Assuming SINR γ_{n_k} follows a log-normal distribution, i.e., $10\log_{10}(\gamma_{n_k})$ is a normal distribution with mean $\mu_{\gamma_{n_k},dB}$ and variance $\sigma^2_{\gamma_{n_k},dB}$, we can find $f_{\gamma_{n_k}}(x)$ by applying the change-of-variables rule on the density function of a normal distribution,

i.e.,

$$f_{\gamma_{n_k}}(x) = \frac{\kappa}{x\sqrt{2\pi\sigma^2_{\gamma_{n_k},dB}}} \exp\left(-\frac{(10\log_{10}(x)-\mu_{\gamma_{n_k},dB})^2}{2\sigma^2_{\gamma_{n_k},dB}}\right)$$

where $\kappa = 10\log_{10}(e)$ and its derivative is given by

$$f'_{\gamma_{n_k}}(x) = -\frac{1}{x} f_{\gamma_{n_k}}(x)\left(1 + \frac{10\log_{10}(x)-\mu_{\gamma_{n_k},dB}}{\sigma^2_{\gamma_{n_k},dB}/\kappa}\right).$$

To prove the concavity of $F_{n_k}(\bar{\gamma}_{n_k}, p_k)$, we require $2f_{\gamma_{n_k}}(\bar{\gamma}_{n_k}) + \bar{\gamma}_{n_k} f'_{\gamma_{n_k}}(\bar{\gamma}_{n_k}) \geq 0$ in (10). That is,

$$f_{\gamma_{n_k}}(\bar{\gamma}_{n_k})\left(1 - \frac{10\log_{10}(\bar{\gamma}_{n_k})-\mu_{\gamma_{n_k},dB}}{\sigma^2_{\gamma_{n_k},dB}/\kappa}\right) \geq 0.$$

It implies $10\log_{10}(\bar{\gamma}_{n_k}) \leq \mu_{\gamma_{n_k},dB} + \sigma^2_{\gamma_{n_k},dB}/\kappa$. This is generally true in a practical system since we usually require the average received SINR $\mu_{\gamma_{n_k},dB}$ to be greater than a QoS threshold $\bar{\gamma}_{n_k}$ (in dB). Moreover, if the average received SINR is far below the QoS threshold, we can have admission control such that the above condition is always satisfied. In Section V via simulation, we find that $\mu_{\gamma_{n_k},dB}$ is in the range of $[-30, 10]$dB depending on SUs' spatial locations while $\sigma_{\gamma_{n_k},dB}$ falls around 25dB. A typical SINR requirement $\bar{\gamma}_{n_k}$ (in dB) for WLAN can be set to 12dB, which is far less than $\mu_{\gamma_{n_k},dB} + \sigma^2_{\gamma_{n_k},dB}/\kappa$.

To study the second-order derivative of PUs' interference with respect to p_k, we define $I_m(\boldsymbol{p}) = \mathbb{E}_{f^w_{\phi_m}}[\mathbf{1}(x \geq \bar{\phi}_m)]$ to be the interference at PU m. If $I_m(\boldsymbol{p})$ is shown to be concave with respect to p_k, so will be $I(\boldsymbol{p})$. Note that $\phi_m = z + p_k h_{km}$ where $z = \sum_{i\neq k} p_i h_{im}$. Letting $f^w_z(\cdot)$ and $f^w_h(\cdot)$ denote the worst-case density function of z and h_{km}, respectively, we have $I_m(\boldsymbol{p}_{-k}, p_k) = 1 - \int_0^{\bar{\phi}_m} f^w_z(y) F^w_h\left(\frac{\bar{\phi}_m - y}{p_k}\right) dy$, where $F^w_h(\cdot)$ denotes the cumulative distribution of $f^w_h(\cdot)$. Consequently,

$$\frac{\partial I_m}{\partial p_k} = \frac{1}{p_k^2}\int_0^{\bar{\phi}_m} f^w_z(y) f^w_h\left(\frac{\bar{\phi}_m - y}{p_k}\right) dy \tag{11}$$

and its second-order derivative is given by

$$\frac{\partial^2 I_m}{\partial p_k^2} = -\frac{1}{p_k^2}\int_0^{\bar{\phi}_m} f^w_z(\bar{\phi}_m - t)\left(2f^w_y(t) + t(f^w_y)'(t)\right) dt \tag{12}$$

where $f^w_y(\cdot)$ denotes the density distribution of $y = p_k h_{km}$. Through a similar reasoning for (10), we have $\frac{\partial^2 I_m}{\partial p_k^2} \leq 0$ if $\bar{\phi}_m(dB) \leq \mu_{y,dB} + \sigma^2_{y,dB}/\kappa$. In the same simulation setting, the critical point $\mu_{y,dB} + \sigma^2_{y,dB}/\kappa$ generally falls in the range $[-30, 10]$dB, which is also much larger than $\bar{\phi}_m$ (in dB). ■

The concavity of $I(\boldsymbol{p}_{-k}, p_k)$ with respect to p_k makes problem (8a)-(8b) difficult to solve directly. As an attempt to transform (8a)-(8b) into an unconstrained optimization problem, we have the Lagrangian function as $\Gamma(\boldsymbol{p}, \nu) = \sum_{k\in\mathcal{K}} u_k(\boldsymbol{p}_{-k}, p_k) - \nu I(\boldsymbol{p}_{-k}, p_k) + \nu\eta$, where ν is the price of interference at PU receivers. Given the price ν, each SAP needs to adjust its transmit power to maximize $\Gamma(\boldsymbol{p}, \nu)$. However, we still face difficulties to solve the problem. Note that both $u_k(\boldsymbol{p}_{-k}, p_k)$ and $I(\boldsymbol{p}_{-k}, p_k)$ are concave functions, and there is no direct way to decouple the interference function $I(\boldsymbol{p})$. To overcome this difficulty, letting $\boldsymbol{\theta} = [\theta_1, \theta_2, \ldots, \theta_K] \succeq 0$, we attribute the total interference $I(\boldsymbol{p})$ to each SAP k by a constant share θ_k, and reformulate the Lagrangian function as follows:

$$\Gamma(\boldsymbol{p}, \nu, \boldsymbol{\theta}) = \sum_{k\in\mathcal{K}} \left[u_k(\boldsymbol{p}_{-k}, p_k) - \nu\theta_k I(\boldsymbol{p}_{-k}, p_k)\right] + \nu\eta. \tag{13}$$

Obviously, we require $\sum_{k\in\mathcal{K}} \theta_k = 1$ and each share θ_k can be viewed as a portion of the total debt to PUs. For different fairness consideration, we can set θ_k accordingly, e.g., we set $\theta_k = 1/K$ to enable equal rights for all SAPs.

To maximize the Lagrangian function (13) in a distributed way, each SAP k optimizes its own transmit power p_k^* according to the overall interference $I(\boldsymbol{p}_{-k}, p_k)$ and its own debt θ_k to PUs, given the knowledge of other SAPs' transmit power $\boldsymbol{p}_{-k}$, i.e.,

$$p_k^*(\nu, \theta_k) = \arg\max_{p_k} u_k(\boldsymbol{p}_{-k}, p_k) - \nu\theta_k I(\boldsymbol{p}_{-k}, p_k). \tag{14}$$

The maximization requires calculations of the first derivatives of $u_k(\boldsymbol{p}_{-k}, p_k)$ and $I(\boldsymbol{p}_{-k}, p_k)$ with respect to p_k. Given the transmit power $\boldsymbol{p}$, we can easily obtain these two derivatives from (9) and (11), respectively. However, we are unable to solve the transmit power p_k^* directly from the first-order optimality condition, i.e., $\partial u_k(\boldsymbol{p}_{-k}, p_k)/\partial p_k = \nu\theta_k \partial I(\boldsymbol{p}_{-k}, p_k)/\partial p_k$, since both sides of this equation are implicit functions of p_k. Note that the worst-case distribution $f^w_z(\cdot)$ in (11) has a form similar to (7) and requires an iterative process to determine its parameters. Therefore, it is very difficult to establish a closed-from relation between $\partial I(\boldsymbol{p}_{-k}, p_k)/\partial p_k$ and p_k. Even though we find such p_k^* from the first-order optimality condition, it is not guaranteed to be the solution as the objective in (14) is a summation of a concave function $u_k(\boldsymbol{p}_{-k}, p_k)$ and a convex function $-\nu\theta_k I(\boldsymbol{p}_{-k}, p_k)$. The resulting p_k^* can be either a local maximum or a local minimum. To this end, we resort to the concave-convex procedure (CCCP) [21] to construct an iterative algorithm that is guaranteed to maximize the objective function monotonically.

Proposition 3: Maximizing $u_k(\boldsymbol{p}_{-k}, p_k) - \nu\theta_k I(\boldsymbol{p}_{-k}, p_k)$ can be performed iteratively by updating power p_k^{t+1}, given current power p_k^t, in a way such that

$$\nabla u_k(\boldsymbol{p}_{-k}, p_k^{t+1}) = \nu\theta_k \nabla I(\boldsymbol{p}_{-k}, p_k^t). \tag{15}$$

Proof: Given any two feasible p_k^t and p_k^{t+1}, the concavity of $u_k(\boldsymbol{p}_{-k}, p_k)$ and $I(\boldsymbol{p}_{-k}, p_k)$ implies the following two inequalities, i.e., $u_k(\boldsymbol{p}_{-k}, p_k^{t+1}) \geq u_k(\boldsymbol{p}_{-k}, p_k^t) - \nabla u_k(\boldsymbol{p}_{-k}, p_k^{t+1})(p_k^t - p_k^{t+1})$ and $-I(\boldsymbol{p}_{-k}, p_k^{t+1}) \geq -I(\boldsymbol{p}_{-k}, p_k^t) - \nabla I(\boldsymbol{p}_{-k}, p_k^t)(p_k^{t+1} - p_k^t)$. It is straightforward to show that, if we have $\nabla u_k(\boldsymbol{p}_{-k}, p_k^{t+1}) = \nu\theta_k \nabla I(\boldsymbol{p}_{-k}, p_k^t)$, the objective function is improved by summing up these two inequalities, i.e., $u_k(\boldsymbol{p}_{-k}, p_k^{t+1}) - \nu\theta_k I(\boldsymbol{p}_{-k}, p_k^{t+1}) \geq u_k(\boldsymbol{p}_{-k}, p_k^t) - \nu\theta_k I(\boldsymbol{p}_{-k}, p_k^t)$. ■

Note that both $\nabla u_k(\boldsymbol{p}_{-k}, p_k)$ and $\nabla I(\boldsymbol{p}_{-k}, p_k)$ are monotonic functions from (9) and (11), respectively. Given p_k^t and $\nabla I(\boldsymbol{p}_{-k}, p_k^t)$, we can use a bisection method to search for p_k^{t+1} satisfying (15). When each SAP tunes to its preferred transmit power, the interference price ν should be updated accordingly. The detailed power control algorithm is given in Algorithm 1. The distribution uncertainties in line 2 of the algorithm are

estimated through channel measurements, and we can update the reference distribution if new measurements reveal that the actual distribution deviates too much from its reference. In line 3 of the algorithm, we can initialize each SAP by its minimum transmit power and choose appropriate interference price ν such that the solution to (14) is nontrivial. Actually, any initial transmit power will not affect the algorithm's convergence to the same point, however, the choice of minimum transmit power will suppress the interference to PUs even during the algorithm iterations. From line 6 to 15, each SAP maximizes its net utility in (14) by the concave-convex procedure. In each iteration, we update SAP's transmit power by a bisection method in lines $9-13$. Then, we increase (or decrease) the interference price ν in line 16 if the resulting power vector $\boldsymbol{p}$ renders higher (or lower) interference than the prescribed level η. The choice of step size α and convergence property of this iterative process can be found in [22].

Algorithm 1 Robust Iterative Power Control

Input: Interference and QoS requirements ϕ_m, η and $\bar{\gamma}_n$
Output: Optimal transmit power $\boldsymbol{p}$ for SAPs

1: **initialization**
2: **estimate** distribution uncertainties $\mathbb{Z}_{\gamma_n}$ and $\mathbb{Z}_{\phi_m}$
3: **set** initial transmit power $\boldsymbol{p}$ and interference price ν
4: **end initialization**
5: For each SAP $k \in \mathcal{K}$
6: **while** $|p_k^{t+1} - p_k^t| > \epsilon$
7: **set** $p_k^t = p_k^{t+1}$ and **calculate** $\nabla I(\boldsymbol{p}_{-k}, p_k^t)$
8: **set** $p_k^U = \bar{p_k}$ and $p_k^L = 0$
9: **while** $|p_k^U - p_k^L| > \epsilon$
10: **if** $\nabla u_k(\boldsymbol{p}_{-k}, \frac{p_k^U + p_k^L}{2}) > \nu\theta_k \nabla I(\boldsymbol{p}_{-k}, p_k^t)$
11: **set** $p_k^L = \frac{p_k^U + p_k^L}{2}$ **else** $p_k^U = \frac{p_k^U + p_k^L}{2}$ **end if**
12: **if** $|\nabla u_k(\boldsymbol{p}_{-k}, \frac{p_k^U + p_k^L}{2}) - \nu\theta_k \nabla I(\boldsymbol{p}_{-k}, p_k^t)| < \epsilon$, **break**
13: **end while**
14: **set** $p_k^{t+1} = \frac{p_k^U + p_k^L}{2}$
15: **end while**
16: **update** price $\nu = [\nu - \alpha(\eta - I(\boldsymbol{p})]^+$ and **go to** line 5

One point worth mentioning is that the calculation of $\nabla I(\boldsymbol{p}_{-k}, p_k^t)$ in line 7 of Algorithm 1 requires the evaluation of $I(\boldsymbol{p}_{-k}, x)$ at two adjacent points, e.g., $x_1 = p_k^t$ and $x_2 = p_k^t + \Delta$. Then we approximate $\nabla I(\boldsymbol{p}_{-k}, p_k^t)$ by $(I(\boldsymbol{p}_{-k}, x_2) - I(\boldsymbol{p}_{-k}, x_1))/\Delta$ for very small Δ compared with p_k^t. By the definition of $I(\boldsymbol{p}_{-k}, p_k^t)$ in (8b), we need to solve another instance of problem (5a)-(5c) by the method developed for Case I. Therefore, from this viewpoint, Case I is the core building block for Case II, not just a routine of simplification.

For implementation of Algorithm 1, we organize it by different functional modules as illustrated in Fig. 3. The information processing module is in charge of the information gathering and synthesis, providing a knowledge profile for the upper operation module to make informed decisions. This module can be further divided into three units. Each SAP's sensing results and operation parameters (e.g., transmit power) are disseminated to other SAPs by the information exchange unit. The uncertainty extraction unit is specially designed for applications in cognitive radio networks. It helps to characterize the range of channel fluctuations by maintaining a reference distribution and a distance limit for every channel gain. When new channel information arrives, the unit calculates the KL divergence with respect to the reference distribution and overwrites the stored distance limit by new KL divergence if it becomes larger. Information sharing among SAPs is usually redundant and requires filtering and restructuring for further processing. In the power control problem, a SAP needs to estimate the interference at PU receivers, which requires the knowledge of SAPs' transmit power and the channel gains from SAPs to specific PU receiver. Therefore, the interference estimation unit will put related information together and provide a worst-case interference estimation based on the uncertainty sets extracted in the preceding unit. It also calculates the change of interference with respect to SAP's transmit power as required in line 7 of Algorithm 1. The information processing module interacts with the robust operation module at the interference estimation unit, which triggers the price update and therefore the power control algorithm. For example, PUs' mobility causes changes of the physical channel condition (as illustrated in Fig. 2) and can be detected by SAPs through overhearing feedback packets from that PU receiver. Then, each SAP updates the uncertainty models and re-evaluates the potential interference to PUs. If current interference estimation is considered low, the robust operation module will suggest to use higher transmit power by tuning down the price of interference.

A distributed implementation of Algorithm 1 would be of paramount significance for practical system. Generally, the distributed design needs to address two problems. The first problem is to decouple secondary network from primary network, limiting information exchange between SAPs and PBS. While the other one is to design a mechanism that enables the information sharing among SAPs. In our model, both power control methods in Case I and Case II do not require any information exchange with the primary network as each SAP can estimate the channel gains between SAP and PU receivers. However, we need some sort of communications among SAPs to estimate the outage probability at PU receivers as given in (4). Assume there is a common control channel among SAPs, then each SAP can collect the channel estimates exchanged from other SAPs and broadcast its own channel estimates as well. After information exchange, each SAP can individually estimate the worst-case outage probability at PU receivers, therefore support a distributed implementation of the power control algorithms. Note that the interference price in Algorithm 1 is a penalty due to interference violation, but it is not necessarily imposed by PBS. Instead, it can be updated and distributed within SAPs through the common control channel.

V. Performance Evaluation

To evaluate the proposed robust power control algorithm, a cognitive radio network with 3 SAPs is simulated under the coverage area of a PBS. The PBS transmits with fixed power at 300mW, and each SAP has a maximum transmit power of 200mW. There are 50 PUs uniformly distributed under PBS's coverage area with radius 800m, and each SAP

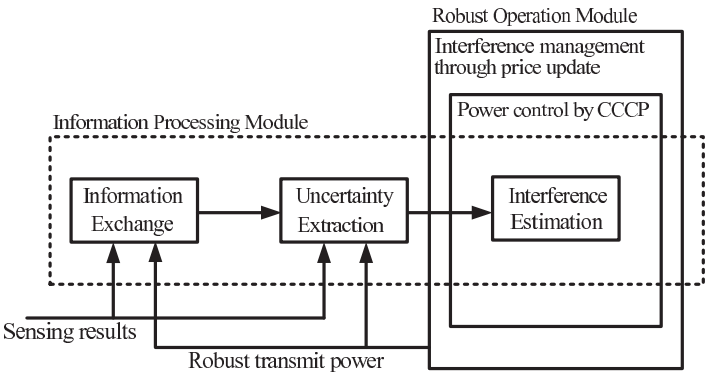

Fig. 3: System structure for robust power control

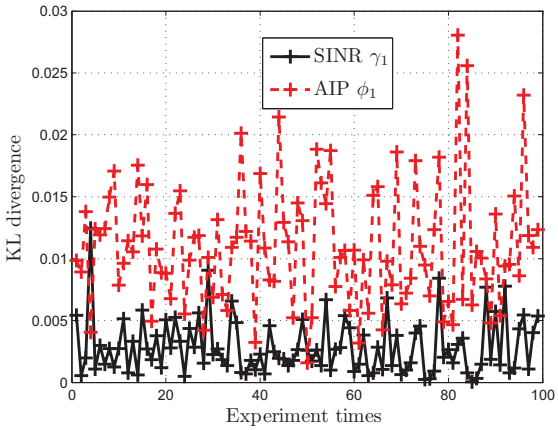

(a) Distribution uncertainty

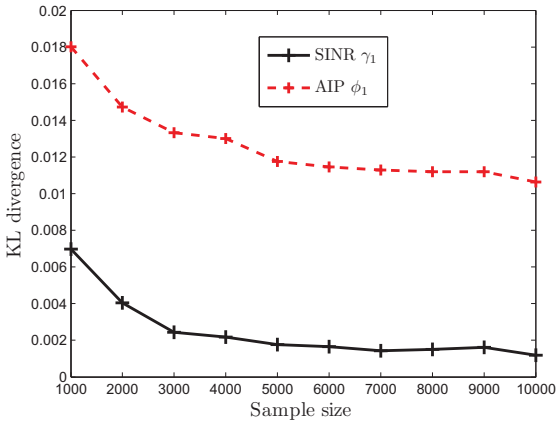

(b) Distance limit vs. sample size

Fig. 4: Empirical setting for distance limit.

has 10 SUs distributed under its coverage area with radius 200m. The placements of SAPs and SUs are at least 30m away from PBS and PUs. The mean path loss is given as $|h|^2 = \frac{1}{cd^n}$ where d is the distance between transceivers, c and n denote the propagation constant and propagation exponent, respectively. Assuming that the primary and the secondary networks experience a similar channel condition, we set the same $c = 0.5$ and $n = 3.5$ for PBS-PU and SAP-SU channels [23], and set a larger $c = 3.5$ for PBS-SU and SAP-PU interference channels. Due to user mobility, the channel gains are subject to log-normal distributed random variables with zero mean and standard derivation 5dB [24]. Each PU receiver has the same interference power threshold $\bar{\phi} = -65$dBw, and the outage probability threshold $\eta = 10\%$. All SUs have the same minimum SINR requirement of 12dB [25], and the noise floor is -130dBw. In the following, we make a comparative study on the performance of our robust methods proposed in Section III and IV, in terms of PU protection levels and QoS provisioning for SUs, respectively. All the simulations are performed in a DELL precision T3500 workstation with Matlab version 7.11.0.584 and Windows 7 Professional SP1.

A. Channel Uncertainty

Before the comparative study, we embody the existence of distribution uncertainty by demonstrating the changes of AIP's and SINR's distribution functions in different channel measurements. As an illustration, we place the PBS at position $(400m, 400m)$, and three SAPs at $(300m, 300m)$, $(300m, 500m)$ and $(750m, 400m)$, respectively. Note that SAPs 1 and 2 are close to each other and to the PBS, while SAP 3 is far away from the PBS. Initially, all SAPs transmit with the same power at 10mW. Based on our channel model, we simulate the channel gain by log-normal distributed random variable on top of the mean path loss, then measure AIPs ϕ_m at PU receivers and SINRs γ_n at SU receivers, respectively. With a limited sample size (e.g., 5000 in the simulations), channel measurements reveal that data samples in each sensing period may follow a distribution other than a log-normal reference distribution. To quantify their difference, we fit the data samples into a closed-form distribution and calculate its KL divergence with respect to the log-normal reference distribution. The results are presented in Fig. 4a. We notice that, compared with SINR, AIP has larger KL divergence with respect to the log-normal reference distribution. This can be shown in our experiments that AIP (in dB) distribution is generally *asymmetric* and has larger skewness than that of SINR (in dB), hence deviates more from its log-normal reference distribution $f^0_{\phi_m}(x)$ which is *symmetric* with respect to $10\log_{10}(x)$. To overcome the distribution uncertainty, we require a distance limit that bounds the KL divergence in most of the cases. Fig. 4b plots an empirical relation between distance limit and the sample size based on the simulation settings. The distance limits in Fig. 4b bound the KL divergence with a probability 90%. Apparently, we need to set a larger distance limit for the AIP distribution than that for the SINR distribution, if we use log-normal reference distributions. In the simulation, we set $D_{\phi_m} = 0.02$ and $D_{\gamma_n} = 0.01$, respectively.

To show the concavity of $u_k(\boldsymbol{p}_{-k}, p_k)$ and $I(\boldsymbol{p}_{-k}, p_k)$ as proved in Proposition 2 with the simulation setting, we plot the changes of $u_k(\boldsymbol{p}_{-k}, p_k)$ and $I(\boldsymbol{p}_{-k}, p_k)$ with respect to p_1 in Fig. 5. When p_1 increases, the average SINR of SUs associated with SAP 1 is correspondingly increased, so does interference at other SU receivers. Therefore, the utility is an increasing function for SAP 1, while a decreasing function for SAPs 2 and 3. Further, we observe that $u_k(\boldsymbol{p}_{-k}, p_k)$ is concave with respect to p_k and convex with respect to other SAPs' transmit power. The

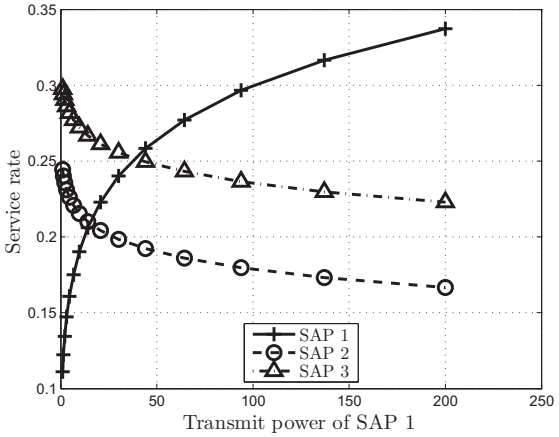

(a) SAP's utility $u_k(\boldsymbol{p}_{-k}, p_k)$.

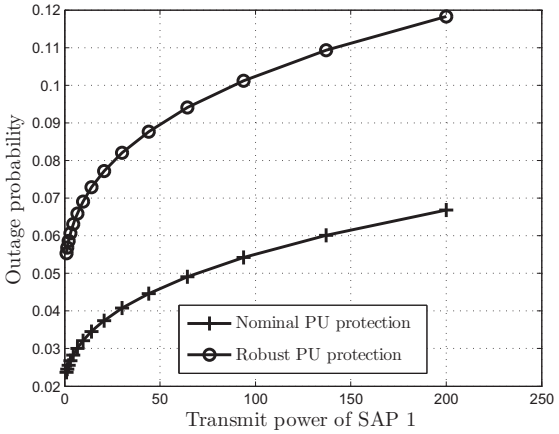

(b) PUs' interference $I(\boldsymbol{p}_{-k}, p_k)$.

Fig. 5: Concavity of $u_k(\boldsymbol{p}_{-k}, p_k)$ and $I(\boldsymbol{p}_{-k}, p_k)$ w.r.t. p_k.

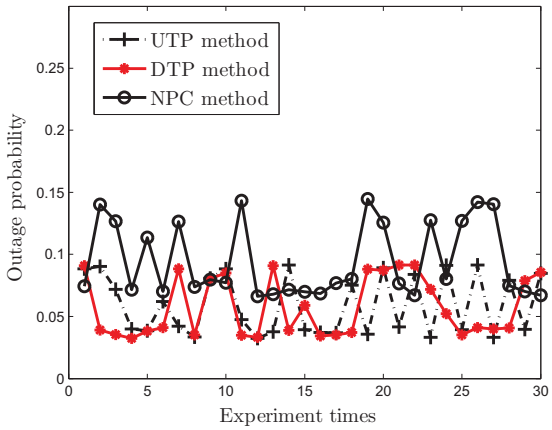

(a) Outage probability at PU receivers

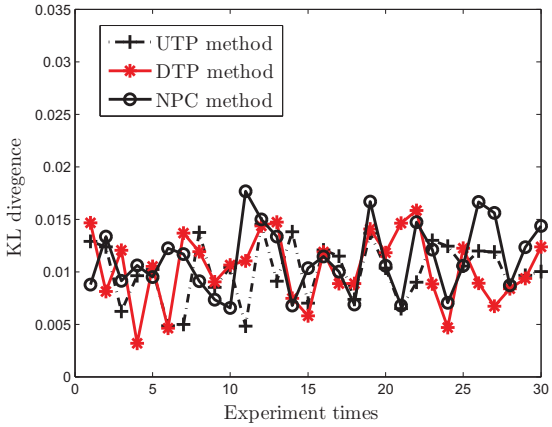

(b) KL divergence in experiments

Fig. 6: PU protection with robust and nominal power control.

concavity of interference function $I(\boldsymbol{p}_{-k}, p_k)$ is illustrated in Fig. 5b where the nominal PU protection is obtained by taking expectation over the reference distribution when calculating the interference $I(\boldsymbol{p}_k, p_k)$. However, with channel uncertainty, the actual outage probability may be much worse than the nominal PU protection level. The robust PU protection level in Fig. 5b gives the worst-case outage probability with a distance limit $D_{\phi_m} = 0.02$.

B. PU Protection

Given the log-normal reference distribution and distance limit, we can obtain the robust transmit power by the proposed algorithms in Sections III and IV. For a clear presentation, we denote these two methods by UTP (universal transmit power) and DTP (distinct transmit power), respectively. To check their protection for PUs, we compare them with a non-robust, i.e., nominal power control method (denoted as NPC) that does not incorporate distribution uncertainty, e.g., [12]. In the NPC method, we simply use the reference distribution as an approximation of the AIP distribution, based on which SAPs estimate the outage probability at PU receivers and adjust their transmit power levels. In our robust methods (UTP or DTP), the AIP may change its distribution in each sensing period and we consider worst-case interference in power control. After we obtain the optimal transmit power from these three methods, we compare the actual interference they introduce to the primary network, respectively.

We have 30 runs in the simulation, and each run contains 500 AIP samples according to the channel fading model, based on which we estimate the outage probabilities at PU receivers. The average outage probability over all PU receivers is given in Fig. 6a. We observe that the robust methods guarantee the outage probability to be less than 10% in all the runs, while the NPC method only provides a desired PU protection level when AIP samples follow a distribution very close to the reference distribution (i.e., small KL divergence in Fig. 6b). However, a violation happens when using the NPC method as the channel fluctuates more intensively and the AIP distribution deviates largely from the reference distribution (i.e. large KL divergence in Fig. 6b). In this case, our robust methods show their significance since the outage probability is still maintained at the prescribed level. Note that the KL divergence in each run is bounded by the empirical distance limit 0.02 as shown in Fig. 6b.

C. SU Performance

With the fluctuations of channel gains, SAP's transmit power may lead to transmission failures due to the violations of PUs' interference constraint. It is likely that, in the case of interference violation, SAPs are forced to suspend their transmissions or levied extra payment for their unsupervised spectrum usage. In the simulation, we set SUs' service rates to zero when PUs' interference constraint is violated, and compare the average service rates with the robust and nominal power control methods, respectively. Each time with different outage probability threshold η, we obtain a nominal transmit power p^N and a robust transmit power p^U from the UTP method, respectively. Then, we run the simulation for 30 times with each of the transmit power, and record the average service rate as shown in Fig. 7a. The results imply that the robust method with UTP may provide more transmit opportunities than that of the NPC method. Even though the NPC method allows SAPs to transmit with higher power and can provide a larger service rate in a single transmission, the high transmit power is vulnerable to punishment from PUs due to potential violations of PUs' interference constraint, and thus brings down SUs' average service rate. We also note that, at $\bar{\phi}_m = -55$dB, SUs' average service rate with the NPC method has a steep raise (Fig. 7a) when the outage probability threshold increases from $\eta = 0.1$ to $\eta = 0.18$, though the transmit power keeps constant at its peak level (Fig. 7b) during this period. That is because, a higher outage probability threshold reduces the probability of transmission failure or punishment from PUs due to the violations of PUs' interference constraint, allowing a very large space for the nominal method to accumulate SUs' average service rate.

Considering SAPs' spatial distribution and their different contributions to the total interference of primary network, we optimize distinct transmit power $\boldsymbol{p}^D = [p_1^D, p_2^D, p_3^D]$ for SAPs by the DTP method, and compare its QoS provisioning for SUs with that of the UTP method. With SAP 3 locating far away, i.e., $(750m, 400m)$ from the center of primary network and inducing less interference, the DTP method enables it to transmit with higher power p_3^D than that of the other SAPs as shown in Fig. 8a, and hence provides a higher service rate than that of UTP method as shown in Fig. 8b. We also compare these two methods when varying SAPs' locations. For simplicity, let SAPs 1 and 2 be stationary and SAP 3 move horizontally from $(500m, 400m)$ to its current location $(750m, 400m)$. Before reaching the location $(600m, 400m)$, SAP 3 has almost the same distance with that of SAPs 1 and 2. Therefore, they have relatively the same interference to PBS, and the DTP method is no better than the UTP method as shown in Fig. 9a. As SAP 3 continues to move away from PBS, the DTP method can notably increase the transmit power of SAP 3, resulting in much higher average transmit power than that of the UTP method as shown in Fig. 9b, and we can observe that the DTP method provides better service rate for SUs.

VI. Conclusions

In this paper, we study the robust power control problem with a new channel uncertainty model. It relies on a reference distribution which is a closed-form approximation extracted from historical channel measurements, while allowing the actual AIP or SINR to follow a different distribution. By using a probabilistic distance measure, we provide a quantitative way to describe the uncertain distribution. Then, we formulate the power control problem into a chance constrained robust optimization, and propose two iterative algorithms to determine the robust transmit power for two cases, respectively. Simulation results demonstrate that both methods provide better PU protection than the existing work which does not take account of channel uncertainty.

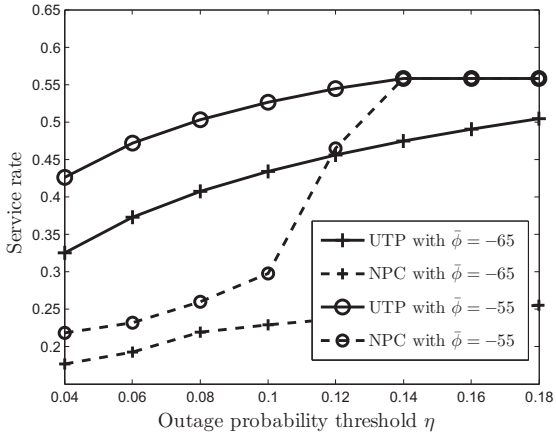

(a) Service rates

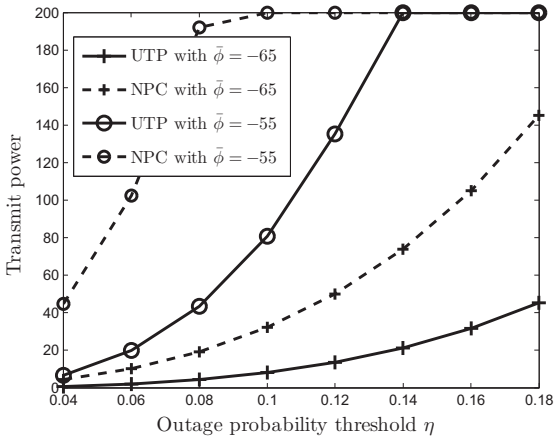

(b) Power levels

Fig. 7: Robust power control vs. nominal power control.

References

[1] S. Haykin, "Cognitive radio: brain-empowered wireless communications," *IEEE J. Sel. Areas Commun.*, vol. 23, no. 2, pp. 201–220, 2005.

[2] S. Gong, P. Wang, and D. Niyato, "Optimal power control in interference-limited cognitive radio networks," in *Proc. IEEE Int. Conf. Commun. Syst. (ICCS)*, pp. 82–86, Nov. 2010.

[3] S. Parsaeefard and A. Sharafat, "Robust worst-case interference control in underlay cognitive radio networks," *IEEE Trans. Veh. Technol.*, vol. 61, pp. 3731–3745, Oct. 2012.

[4] S. Gong, X. Chen, J. Huang, and P. Wang, "On-demand spectrum sharing by flexible time-slotted cognitive radio networks," in *Proc. IEEE Globecom*, Dec. 2012.

[5] X. Chen and J. Huang, "Distributed spectrum access with spatial reuse," *CoRR*, vol. abs/1209.5130, 2012.

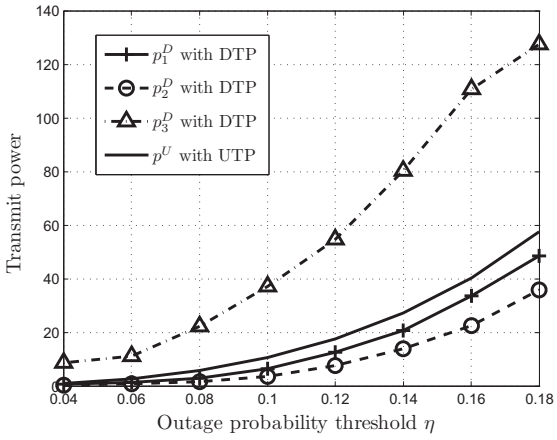

(a) Power levels

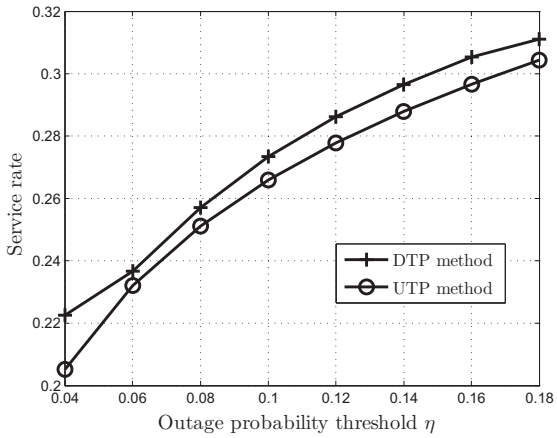

(b) Service rates

Fig. 8: The comparison between robust UTP and DTP methods.

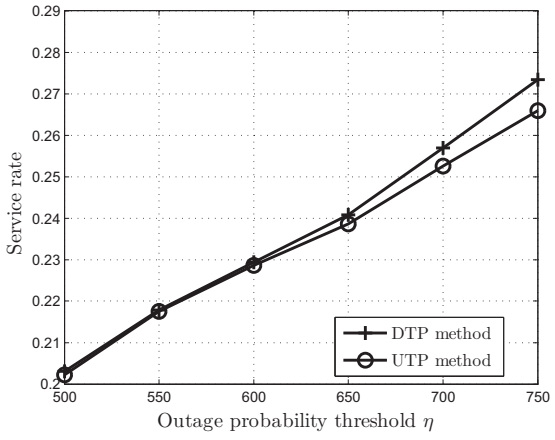

(a) Service rates

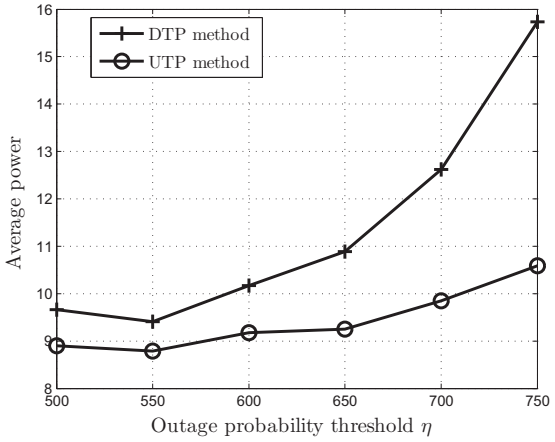

(b) Average power

Fig. 9: Performance comparison as SAP 3 moving away from PBS.

[6] A. Konrad, B. Y. Zhao, A. D. Joseph, and R. Ludwig, "A Markov-based channel model algorithm for wireless networks," *Wireless Networks*, vol. 9, pp. 189–199, May 2003.

[7] W. Ren, Q. Zhao, and A. Swami, "Power control in cognitive radio networks: how to cross a multi-lane highway," *IEEE J. Sel. Areas Commun.*, vol. 27, pp. 1283–1296, Sep. 2009.

[8] S. Huang, X. Liu, and Z. Ding, "Distributed power control for cognitive user access based on primary link control feedback," in *Proc. IEEE INFOCOM*, pp. 1–9, Mar. 2010.

[9] S. Huang, X. Liu, and Z. Ding, "Decentralized cognitive radio control based on inference from primary link control information," *IEEE J. Sel. Areas Commun.*, vol. 29, no. 2, pp. 394–406, 2011.

[10] G. Zheng, S. Ma, K.-K. Wong, and T.-S. Ng, "Robust beamforming in cognitive radio," *IEEE Trans. Wireless Commun.*, vol. 9, no. 2, pp. 570–576, 2010.

[11] J. Proakis, *Digital Communications*. McGraw-Hill, Aug. 2000.

[12] E. Dall'Anese, S.-J. Kim, G. Giannakis, and S. Pupolin, "Power control for cognitive radio networks under channel uncertainty," *IEEE Trans. Wireless Commun.*, vol. 10, no. 10, pp. 3541–3551, 2011.

[13] G. Zheng, K.-K. Wong, and B. Ottersten, "Robust cognitive beamforming with bounded channel uncertainties," *IEEE Trans. Signal Process.*, vol. 57, pp. 4871–4881, Dec. 2009.

[14] Y. Huang, Q. Li, W.-K. Ma, and S. Zhang, "Robust multicast beamforming for spectrum sharing-based cognitive radios," *IEEE Trans. Signal Process.*, vol. 60, no. 1, pp. 527–533, 2012.

[15] Z. Chen, C.-X. Wang, X. Hong, J. Thompson, S. Vorobyov, X. Ge, H. Xiao, and F. Zhao, "Aggregate interference modeling in cognitive radio networks with power and contention control," *IEEE Trans. Commun.*, vol. 60, pp. 456–468, Feb. 2012.

[16] K. Chowdhury and I. Akyldiz, "OFDM-based common control channel design for cognitive radio ad hoc networks," *IEEE Trans. Mobile Comput.*, vol. 10, no. 2, pp. 228–238, 2011.

[17] W.-H. Chung and K. Yao, "Modified hidden semi-Markov model for modelling the flat fading channel," *IEEE Trans. Commun.*, vol. 57, no. 6, pp. 1806–1814, 2009.

[18] R. M. Gray, *Entropy and Information Theory*. Springer-Verlag New York, Inc., 1990.

[19] Y. Shi, Y. T. Hou, and H. Zhou, "Per-node based optimal power control for multi-hop cognitive radio networks," *IEEE Trans. Wireless Commun*, vol. 8, pp. 5290–5299, Oct. 2009.

[20] A. Quarteroni, R. Sacco, and F. Saleri, *Numerical Mathematics*. Texts in Applied Mathematics, Paris, FR: Springer, 2007.

[21] A. Yuille and A. Rangarajan, "The concave-convex procedure," *Neural Comput.*, vol. 15, pp. 915–936, Apr. 2003.

[22] D. P. Bertsekas and J. N. Tsitsiklis, *Parallel and Distributed Computation: Numerical Methods*. Athena Scientific, 1997.

[23] J. Sachs, I. Maric, and A. Goldsmith, "Cognitive cellular systems within the TV spectrum," in *Proc. IEEE DySPAN*, pp. 1–12, Apr. 2010.

[24] W. Kumwilaisak and C.-C. J. Kuo, "Adaptive variable length Markov chain for non-stationary fading channel modeling," in *Proc. IEEE Globecom*, pp. 2046–2050, Nov. 2002.

[25] H. Islam, Y.-C. Liang, and A. Hoang, "Joint power control and beamforming for cognitive radio networks," *IEEE Trans. Wireless Commun.*, vol. 7, pp. 2415–2419, Jul. 2008.